Asia-Pacific Journal of Atmospheric Sciences (2019) 55:415–427
https://doi.org/10.1007/s13143-019-00105-0

Online ISSN 1976-7951
Print ISSN 1976-7633

ORIGINAL ARTICLE

Comparison of XCH_4 Derived from g-b FTS and GOSAT and Evaluation Using Aircraft In-Situ Observations over TCCON Site

Samuel Takele Kenea[1] · Young-Suk Oh[1,2] · Tae-Young Goo[1] · Jae-Sang Rhee[1] · Young-Hwa Byun[1] · Lev D. Labzovskii[1] · Shanlan Li[1]

Received: 18 February 2018 / Revised: 31 December 2018 / Accepted: 17 January 2019 / Published online: 28 February 2019

Abstract
It is evident that evaluating the measurement of greenhouse gases (GHGs) obtained from multi-platform instruments against accurate and precise instrument such as aircraft in-situ is very essential when using remote sensing GHGs results for source/sink estimations with inverse modeling. The results of the inverse models are very sensitive even to small biases in the data (Rayner and O'Brien 2001). In this work, we have evaluated ground-based high resolution Fourier Transform Spectrometer (g-b FTS) and the Greenhouse gases Observing SATellite (GOSAT) column-averaged dry air mole fraction of methane (XCH_4) through aircraft in-situ observations over Anmyeondo station (36.538° N, 126.331° E, 30 m above sea level). The impact of the spatial coincidence criteria was assessed by comparing GOSAT data against g-b FTS. We noticed there was no any systematic difference based on the given coincidence criteria. GOSAT exhibited a bias ranging from 0.10 to 3.37 ppb, with the standard deviation from 4.92 to 12.54 ppb, against g-b FTS with the spatial coincidence criteria of ±1, ±3, ±5 degrees of latitude and longitude and ± 1 h time window. Data observed during ascent and descent of the aircraft is considered as vertical profiles within an altitude range of 0.2 to a maximum of 9.0 km so that some assumptions were applied for the construction of the profiles below 0.2 and above 9.0 km. In addition, the suitability of aircraft data for evaluation of remote sensing instruments was confirmed based on the assessment of uncertainties. The spatial coincidence criteria is ±1° latitude and ± 2° longitude and for temporal difference is ±1 h of the satellite observation overpass time were applied, whereas g-b FTS data are the mean values measured within ±30 min of the aircraft observation time. Furthermore, the sensitivity differences of the instruments were taken into account. With respect to aircraft, the g-b FTS data were biased by −0.19 ± 0.69%, while GOSAT data were biased by −0.42 ± 0.84%. These results confirm that both g-b FTS and GOSAT are consistent aircraft observations and assure the reliability of the datasets for inverse estimate of CH_4.

Keywords Aircraft in-situ · G-b FTS · GOSAT · XCH_4

1 Introduction

Next to CO_2, atmospheric methane (CH_4) is one of the potent greenhouse gases. Its concentrations have been increasing since pre-industrial era as a result of intense human activities such as burning of fossil fuel and changes in land use. CH_4 plays a major role in the chemistry of the Earth's atmosphere through the decomposition process; its increase is considered to change the balance of related chemical species (Cicerone and Oremland, 1998). Therefore, accurate and precise measurements of CH_4 play a substantial role for better comprehension in global carbon cycle as well as its contribution to the global warming (Jain et al. 2000). Even though CH_4 is the dominant anthropogenic greenhouse gas, there are still high uncertainties in CH_4 sources and sinks at a global scale (Frankenberg et al. 2008). A number of instruments deployed onboard at various platforms (ground-based, airborne, and space-borne) have been involved in measuring of atmospheric concentrations of CH_4. Aircraft in-situ measurements are highly accurate and precise and, therefore, capable to validate the ground-based instruments such as g-b FTS, as well as

Responsible Editor: Soon-Il An.

✉ Samuel Takele Kenea
samueltake@yahoo.ca

[1] Climate Research Division, National Institute of Meteorological Sciences (NIMS), 33, Seohobuk-ro, Seogwipo-si, Jeju-do 63568, Republic of Korea

[2] Department of Electrical Eng. and Center for Edge Plasma Science, Hanyang University, Seoul, Republic of Korea

evaluate satellites instruments such as GOSAT. However, aircraft observations are very sparse; this gap needs to be filled by highly accurate and precise measurements from satellite. Several studies on validation of remote sensing products of greenhouse gases such as CO_2 and CH_4 were conducted based on aircraft in-situ measurements at various sites (Araki et al. 2010; Messerschmidt et al. 2011; Geibel et al. 2012; Tanaka et al. 2012; Miyamoto et al. 2013; Inoue et al. 2013, 2014). The satellite products of CH_4 should attain a demanding precision of <2% (< 34 ppb), in order to improve the precision of inversion models. In addition, achieving high relative accuracy (< 10 ppb for XCH_4) is more crucial and demanding than precision to derive reliable surface fluxes via inverse modelling (Buchwitz et al. 2016).

In this study, we have addressed two major issues. First, observations of XCH_4 and comparison between GOSAT and g-b FTS XCH_4 observations over the Anmyeondo station are discussed. Second, we assessed the suitability of aircraft in-situ observations for validating other datasets and then evaluate the correlative remote sensing measurements (g-b FTS and GOSAT) against aircraft. Here, the aircraft in-situ XCH_4 was computed based on the approach suggested by Inoue et al. (2013) and Ohyama et al. (2015). In fact, our g-b FTS was calibrated with respect to TCCON (Total Carbon Column Observing Network) common scale factor which is basically derived from the aircraft data made at the other TCCON sites, therefore, our study will be useful for the scale factor examination for Anmyeondo station by increasing the number of sample size. This paper is organized as follow: Section 2 gives short descriptions about the Anmyeondo station. A brief overview of data and method is provided in Section 3. Section 4 presents results and discussion and followed by conclusions in Section 5.

2 The Anmyeondo Station

The Anmyeondo station is located at 36.538 °N, 126.331 °E, and 30 m above sea level. The topographic feature of the Anmyeondo station is a complex terrain which consists of hills and valley within a few hundred meters. The climatic condition of the site is categorized as: winter is the coldest season (a minimum temperature is about 2.7 °C) while summer is the warmest season (a maximum temperature is about 25.6 °C), (the Anmyeondo station description is also given in Oh et al. (2018) paper). In other aspects, industries are available within 100 km of the station. This area consists of agriculture, forests, and urban areas. Several instruments are being operated at the Anmyeondo station which makes this site is important for validating remote sensing products from different platforms such as GOSAT. Figure 1 depicts all TCCON sites (including operational, future, and previous sites) globally.

3 Data and Methods

3.1 Aircraft Measurements

To provide in-situ measurements of atmospheric CO_2, CH_4, CO, and H_2O concentrations, the aircraft was equipped with a Wavelength-Scanned Cavity Ring Down Spectrometer (CRDS; Picarro, G2401-mc) providing mixing ratio data recorded at ~0.3 Hz intervals. The position (latitude, longitude, and height) of the aircraft was monitored by GPS, and information on the outside temperature, static pressure, and ground speed was provided by the aircraft's instruments. Figure 2 displays schematic views of the CRDS instruments. Data collected during ascent and descent of the aircraft is considered as vertical profiles of CH_4 over the Anmyeondo station. Typical durations are in the range of 0.5–3 h. The temperature and pressure of the gas sample have to be tightly controlled at 45 °C and 140 Torr in the CRDS (variations of less than 20 mK and 0.1 Torr, respectively), which leads to highly stable spectroscopic features (Chen et al. 2010). Any deviations from these values cause a reduction of the instrument's precision. Data recorded beyond these range of variations in cavity pressure and temperature were discarded in this analysis. Variance of the cavity pressure and temperature during flight results in noise in the CH_4 mixing ratios. The Picarro CRDS instrument has been regularly calibrated with respect to the standard gases within the error range recommend by WMO.

3.2 In-Situ Observation Data

As for complementary information below the lower boundary of the aircraft observation, we utilized the CH_4 concentration data measured by the meteorological tower in the Anmyeondo site (36.53 °N, 126.32 °E, and 47 m above sea level), in close vicinity to the TCCON station. Atmospheric concentrations of CH_4 at 86 m above sea level were continuously measured with a precision <2 ppb using CRDS and provided as hourly averaged data. Sensors for detection of wind speed and direction, air temperature, barometric pressure, and humidity have been also installed at this height. The in-situ data closest to the aircraft measurement time were selected to complement CH_4 profiles. These data can be obtained from the WMO World Data Center for Greenhouse Gases (WDCGG) (http://ds.data.jma.go.jp/gmd/wdcgg/catalogue.cgi).

3.3 Ground-Based FTS

The g-b FTS has been operating at Anmyeondo station within the network of TCCON since 2014; and detailed information about g-b FTS at this station was recently reported in Oh et al. (2018). The TCCON is a worldwide network of ground-based FTSs that was founded in 2004. It has been widely used as a calibration and validation resource for satellite measurements

Fig. 1 Global distributions of the TCCON sites. (https://tccondata.org/)

(e.g. Morino et al. 2011), but it is also offered for better understanding of the carbon cycle (e.g. Yang et al. 2007). The g-b FTS provides spectra in the near infrared spectrum with a high spectral resolution of 0.02 cm^{-1} and a temporal resolution of ~2 min. From the recorded spectra, the target species (XCH_4) was retrieved with the GFIT nonlinear least-squares fitting algorithm, which verifies a vertical scale factor (γ) of an a priori vertical profile based on the best spectral fit of the solar absorption signal. The scaled profile is then vertically integrated, and the resulting column abundance is divided by the vertical column of dry air, calculated using the retrieved column of oxygen (O_2) (Wunch et al. 2011).

3.4 Greenhouse Gases Observing SATellite (GOSAT)

GOSAT was launched into a sun-synchronous orbit on 23 January 2009 by H-IIA launch vehicle. It was placed in a sun-synchronous orbit at a 666-km altitude and has a 3-day revisit orbit cycle and a 12-day operation cycle. It carries two sensors: the TANSO-FTS (Thermal And Near-infrared Sensor for carbon Observation Fourier Transform Spectrometer) and TANSO-CAI (TANSO Cloud and Aerosol Imager) with the IFOV of 10.5 km and 0.5–1.5 km, respectively. The TANSO-FTS onboard GOSAT makes global observations both at nadir and off-nadir modes; and makes use of four spectral bands for deriving CO_2 and CH_4 (Kuze et al. 2009) accurately. The TANSO-FTS records the solar radiation reflected from the surface at three Short Wavelength InfraRed (SWIR) bands at the respective wavelength of 0.76, 1.6, and 2.0 μm and the Earth's radiation from the surface and atmosphere at the wide Thermal InfraRed (TIR) band which is in the range between 5.5 and 14.3 μm with a resolution of 0.2 cm^{-1}. The retrieval algorithm is a non-linear maximum a posteriori method with linear mapping based on Rodgers (2000). In this work, we have used column-averaged dry air mole fractions of CH_4 (XCH_4) V022 derived from the NIES retrieval algorithm (Yoshida et al. 2011, 2013). The achieved single measurement precision (random error) of the GOSAT XCH_4 is

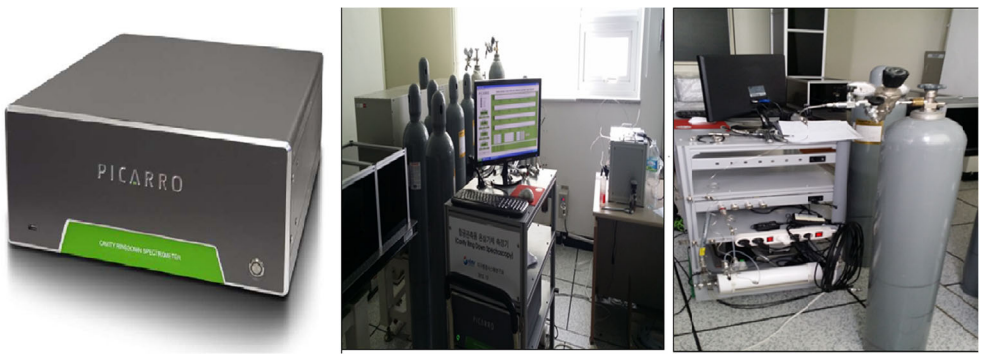

Fig. 2 Left panel is CRDS instrument and right panel depicts the CRDS laboratory including gas cylinders for calibration purposes and computer

approximately 16 ppb (1.0%) while systematic errors (relative accuracy or relative bias) are approximately 6 ppb (0.3%) (Buchwitz et al. 2016). We accessed the GOSAT data through website (https://data2.gosat.nies.go.jp).

3.5 Methods

The vertical profiles of CH_4 mixing ratio are obtained during ascent and descent of the aircraft in spiral path (see Fig. 3) over Anmyeondo station. Since the altitude range of the aircraft measurements were limited to approximately 0.2–5.0 km from 2012 to 2016 aircraft campaign and the maximum flight altitude was 9.0 km in 2017, the in-situ data were utilized near the surface to complement the CH_4 profiles of aircraft-based data, while above the aircraft ceiling, the highest altitude of the aircraft observation data were extended up to the tropopause level to construct the complete CH_4 profiles in a similar way as proposed by Miyamoto et al. (2013); Ohyama et al. (2015). We have used the in-situ data at the surface level to complement the aircraft profile. Local planetary boundary layer (PBL) heights were obtained from National Centers for Environmental Prediction (NCEP) NOAA (National Oceanic and Atmospheric Administration) reanalysis data. The mole fractions between the uppermost aircraft measurement and the tropopause are assumed to be maintained constant as the highest aircraft measurements because at these higher altitudes the air is well mixed. For this analysis, the tropopause height was determined from European Center for Medium range Weather Forecasting (ECMWF) ERA-Interim reanalysis data, a horizontal resolution of 0.75×0.75 degrees. Above the tropopause height, GFIT a priori profiles were fixed to the aircraft data as shown by black dashed line in the left panel of Fig. 4. The dry air number density profiles derived from radiosonde observation and ERA-Interim reanalysis data were utilized for the calculation of the total column amounts of CH_4. The total column amounts of CH_4 were numerically integrated from the in-situ aircraft profiles weighted by dry air density from the surface up to the altitude of 70 km using the following equation (e.g., Tanaka et al. 2012):

$$VC_s = \int_0^{P_s} \frac{f_{CH_4}^{dry}\left(1-f_{H_2O}\right)}{g.\mathrm{m}} dp \quad (1)$$

where P_s is surface pressure, f_{H_2O} - mole fraction of H_2O, f_{CH_4} - mole fraction of CH_4, m – molecular mass of air, and g - gravitational acceleration. The column averaged dry-air mole fractions of CH_4 are calculated from the integrated column amounts using the equation given below:

$$XCH_4 = \frac{column\ CH_4}{column\ air} \quad (2)$$

where XCH_4 is the column-averaged dry-air mole fraction of CH_4. We set the coincidence criteria for comparison between satellite data (GOSAT) and aircraft data as follows: GOSAT data are considered within ±1 degree latitude and ± 2 degree longitude boxes centered at the Anmyeondo station and the aircraft data temporally nearest to the GOSAT overpass time were selected, a maximum of 1 h difference. While the g-b FTS data were averaged within ±30 min of the aircraft overpass, which reduce the random error. During validation of remote sensing vertical profiles, it is reasonable to consider the effect of vertical resolution and sensitivity of the data (Rodgers and Connor 2003). In this analysis, vertically highly resolved aircraft CH_4 profiles were degraded by applying the column averaging kernels (a_j) of low resolution of vertical profiles derived from the

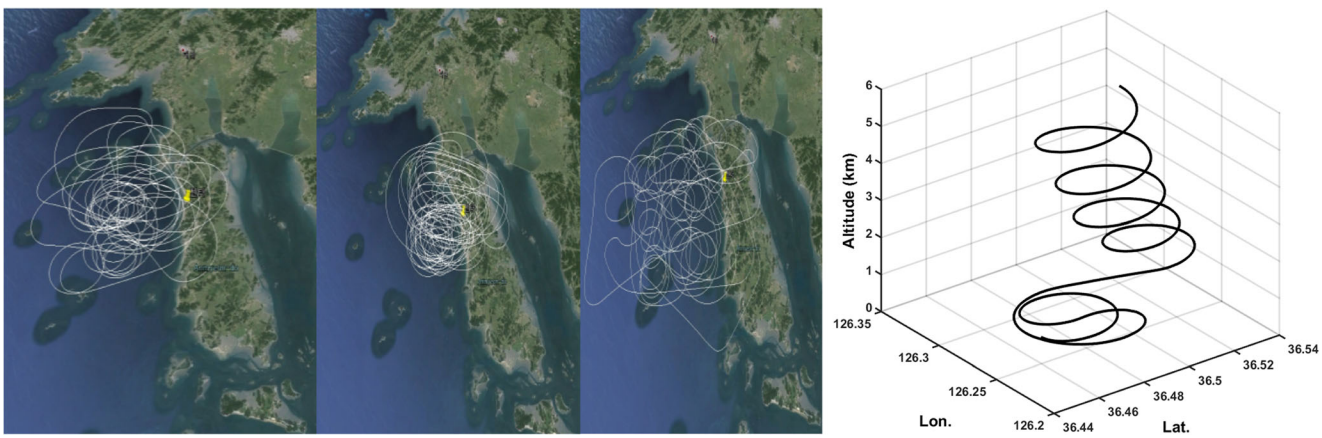

Fig. 3 Typical flights path of the aircraft taken on May 09, 10, and 16, 2015 from left to right panels, respectively, are depicted. The right panel depicts vertical spiral flight path over Anmyeondo

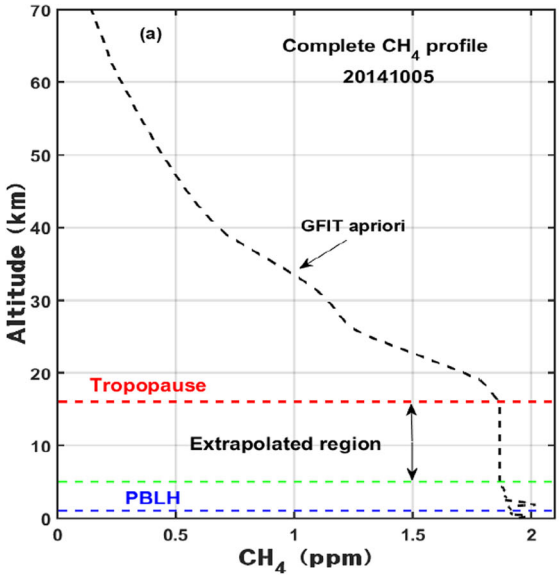

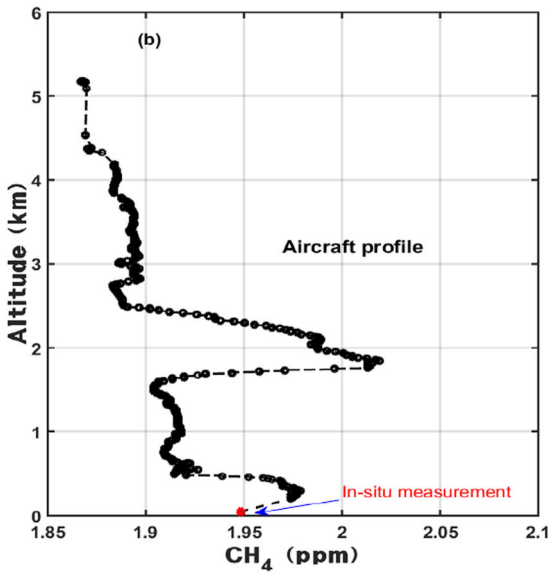

Fig. 4 The left and right panels display the complete CH_4 profile and aircraft profile appended with surface measurements, respectively, October 05, 2014. The red and blue broken lines represent the tropopause and planetary boundary heights, respectively, and green broken line shows the maximum aircraft observation altitude

remote sensing instruments based on the following equation:

$$XCH_4^{in-situ} = XCH_4^a + \sum_j h_j a_j (t_{in-situ} - t_a) \quad (3)$$

where $XCH_4^{in-situ}$ is the column-averaged dry-air mole fraction of CH_4 from the aircraft in-situ measurement, XCH_4^a and t_a are a priori column-averaged dry-air mole fraction and profile of CH_4, respectively (from g-b FTS or GOSAT), h_j is the pressure weighting function, and $t_{in-situ}$ is the in-situ profile from aircraft measurement. The averaging kernel for the column retrieval is a vector representing the sensitivity of the retrieved total column to perturbations of the partial columns at the various atmospheric levels. The typical column-averaging kernels for the g-b FTS and GOSAT at the Anmyeondo station are shown in Fig. 5. The differences of XCH_4 between the aircraft and the remote sensing instruments or between g-b FTS and GOSAT are expressed in terms of absolute and relative differences and the following mathematical expressions are:

$$\text{Abso.diff.} = X_{ins} - X_{in-situ/FTS} \quad (4)$$

$$\text{Rel.diff.} = 100\% \frac{(X_{ins} - X_{in-situ/FTS})}{X_{in-situ/FTS}} \quad (5)$$

where $X_{in-situ/FTS}$ and X_{ins} are XCH_4 of the aircraft and the correlative remote sensing instruments (g-b FTS and GOSAT) or g-b FTS and GOSAT (which is used for the comparison between g-b FTS and GOSAT), respectively. We examined the weather conditions at the measurement station during all observation periods. For this period, we showed meteorological parameters such as relative humidity, temperature, wind speed, and wind direction from radiosonde data in Fig. 6 in order to speculate the weather conditions at the Anmyeondo station. Approximately above 3 km, the amount of atmospheric moisture was very low which was depicted by the relative humidity (RH) of below 40% in Fig. 6(a). As shown in panels c and d of Fig. 6, the northerly and north easterly winds was blowing with a magnitude of lower than 8 m s^{-1} below 2 km, whereas between 2 and 6 km, the westerly and north westerly winds advected at a maximum speed of 20 m s^{-1} over the measurement station. Therefore, this could bring a continental air mass from the Northern Hemisphere to the Anmyeondo station.

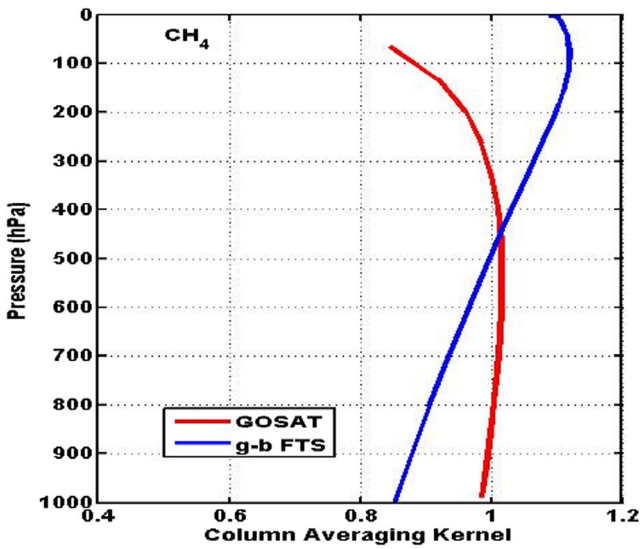

Fig. 5 Column Averaging Kernels (CAKs) of CH_4 are shown

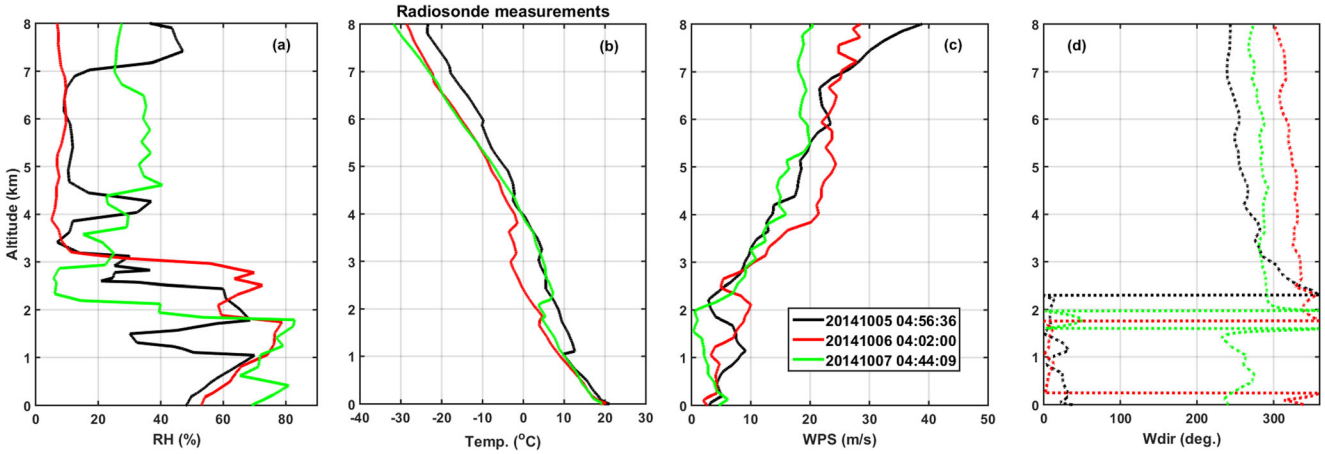

Fig. 6 Radiosonde measurements of (**a**) relative humidity, (**b**) temperature, (**c**) wind speed, and (**d**) wind direction, taken on October 05–07, 2014

4 Results and Discussion

In the following subsections, we have discussed observations and comparison of XCH_4 between g-b FTS and GOSAT, and then evaluated them based on the aircraft in-situ observations.

4.1 Observations of XCH_4 and Comparisons between g-b FTS and GOSAT

Here, the time series of XCH_4 comparison between g-b FTS and GOSAT was performed in the period between 2014 and 2016 (see Fig. 7). We assessed to what extent

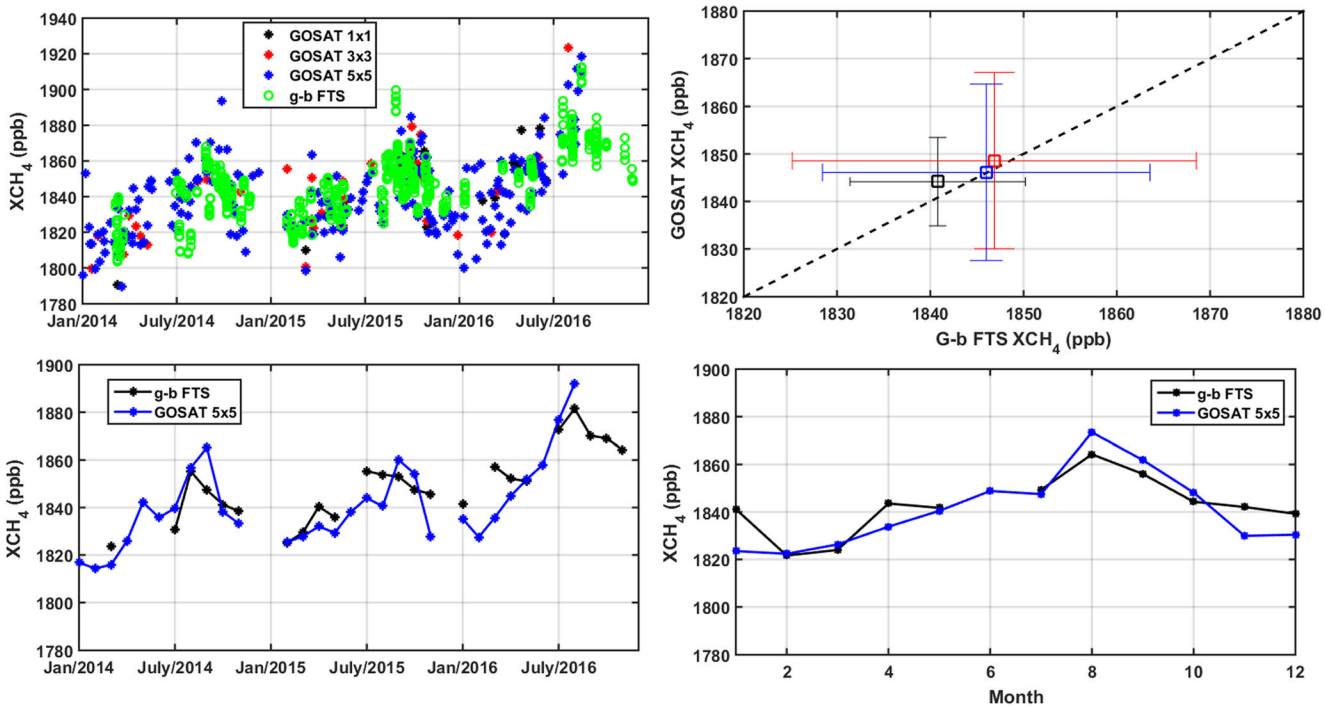

Fig. 7 Time series of XCH_4 obtained from the g-b FTS and the GOSAT (left top panel) and GOSAT versus g-b FTS (right panel) in the period of 2014 to 2016 with a one-to-one dashed line, green circle denotes hourly mean values of the g-b FTS, while the asterisks represent single day observations of the GOSAT. Right top panel shows g-b FTS vs GOSAT at the spatial coincidence criteria of ±1, ±3, ±5 degrees latitude/longitude green, blue, and red colors, respectively, and error bars indicate the standard deviations of the coincident datasets. Bottom left panel shows the time series of XCH_4 on monthly mean basis and bottom right panel depicts annual cycle 2014–2016

Table 1 Statistical results for the XCH_4 difference between GOSAT and g-b FTS (bias = GOSAT - g-b FTS) data based on coincidence criteria of ±1, ±3, and ± 5 degrees of lat/lon and ± 1 h. N = number of coincident data, R = correlation coefficient

Lat./ lon.(deg)	N	R	RMSE (ppb)	bias ± std. (ppb)	Rel. diff. ± std. (%)
±1	9	0.86	5.73	3.37 ± 4.92	0.18 ± 0.27
±3	16	0.96	6.01	1.68 ± 6.00	0.09 ± 0.33
±5	27	0.76	12.31	0.10 ± 12.54	0.01 ± 0.68

the impact of spatial coincidence criteria affects the comparison results. To match up the GOSAT data against g-b FTS, we chose geometric coincidence criteria of ±1, ±3, and ± 5 degrees of latitude/longitude centered at the Anmyeondo station within the temporal window of ±1 h. Following the match-ups, all g-b FTS data coinciding with one satellite observation which were within 1 h time window are averaged, minimizing the g-b FTS random error. As a result of those coincidence criteria, we obtained different sample size that might also affect the statistics to have robust conclusion. As can be seen in the top left panel of Fig. 7, the overall results suggested that both instruments agreed in capturing the seasonal variability of XCH_4 over the Anmyeondo station. Relatively large discrepancies were detected in peak methane season, summer which might reflect the high spatial heterogeneity of methane source and sink strength (details are beyond the scope of this paper). The seasonal and annual cycles of XCH_4 derived from the GOSAT were compared with in g-b FTS observations over the Anmyeondo station, which are provided in the bottom panels of Fig. 7. Because of sample size, we used GOSAT data that extracted within ±5 degrees latitude/longitude coincidence criteria. As can be seen in Fig. 7 bottom panels, the overall patterns of seasonal and annual cycle of the g-b FTS XCH_4 are reproduced by GOSAT XCH_4. The maximum and minimum amounts of methane were observed during summer and winter seasons, respectively. However, the seasonal cycle of CH_4 in the Northern Hemisphere is more complex (Dlugokencky et al. 1994). While the destruction of CH_4 due to reaction with OH is expected to be stronger in summer, source strengths also strongly vary with the seasons. East Asia is one of the largest source regions of methane, and enhanced concentrations over this region are predicted by model studies (Houweling et al. 2000). Dlugokencky et al. (1993) reported that significantly elevated CH_4 mixing ratio was observed at Tae-ahn Peninsula, Korea (36° 44' N, 126° 08′ E) during summer correlated with northwesterly airflow from northeast China and east Siberia. In fact, taking a coarse collocation criteria can induce collocation errors, but considering a very strict criterion leads to a small sample set (which affects statistics) due to the sparseness of GOSAT soundings. Buchwitz et al. (2017) described the spatial variability in the bias of XCH_4 termed as "relative bias". It can arise from different surface reflectivity, aerosol interference, and sloping terrain. They estimated 10 ppb relative bias for solar backscatter satellite observations. Correlations, root mean square error (RMSE), bias, and relative differences for these comparisons are detailed in Tables 1 and 2 for varying collocation criteria. As RMSE values increases from 5.73 to 12.31 ppb with increasing the spatial window ±1 to ±5 degrees, which cover land and ocean parts since the Anmyeondo station is located at the coastal area. In general, there was no systematic difference noticed by changing the collocation space. It was found low bias (±σ) in GOSAT XCH_4 against g-b FTS, which is about 3.37 ± 4.92 ppb, with a corresponding relative difference of 0.18 ± 0.27%, when applying the strict collocation criteria within a time window of ±1 h and ± 1 degree of latitude/longitude (see Table 1). Since we set the same time window but changing the spatial window by ±3 and ± 5 degrees that resulted in the mean bias of 1.68 ± 6.0 and 0.10 ± 12.54 ppb, respectively. The standard deviations of the differences are progressively increasing as increasing the collocation space, but those values are

Table 2 The same as Table 1, but for daily mean basis. (bias = GOSAT minus g-b FTS)

Lat./lon.(deg)	N	R	RMSE (ppb)	bias ± std. (ppb)	Rel. diff. ± std. (%)
±1	12	0.80	6.10	0.77 ± 6.30	0.04 ± 0.34
±3	20	0.90	8.30	1.68 ± 8.34	0.09 ± 0.45
±5	35	0.79	10.90	0.36 ± 10.98	0.04 ± 0.60

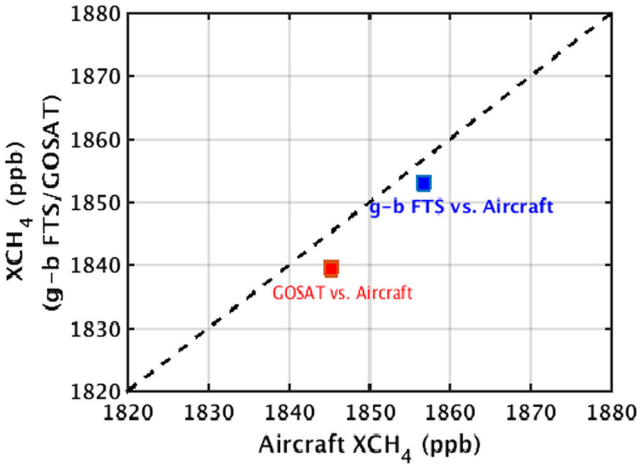

Fig. 8 The comparisons of XCH_4 between the aircraft observation versus g-b FTS data (represented by blue square) and GOSAT (denoted by red square) over Anmyeondo station are shown. The dashed line shows one-to-one line

compatible with the combined measurement errors of the instruments. Similarly, we investigated the impact of the coincidence criteria by setting the time window on daily mean basis of g-b FTS measurements of XCH_4 with varying the spatial coincidence ±1, ±3, and ± 5 degrees of latitude/longitude, and the bias was estimated to be less than 1.68 ppb. For a case of ±1 degree latitude/longitude, GOSAT was biased by 0.78 ± 6.3 ppb with respect to g-b FTS. Those values are within the range of validation results reported in previous findings (e.g. Yoshida et al. 2013; Gavrilov et al. 2014; Ohyama et al. 2015) but with slightly smaller biases. Yoshida et al. (2013) performed a validation of GOSAT XCH_4 (V02.xx) using the 723 measurements provided by TCCON and showed that bias was −5.90 ± 12.6 ppb. Gavrilov et al. (2014) compared GOSAT XCH_4 (V02.xx) with 256 ground-based FTS measurements ob-

Table 3 Summary for the statistics of XCH_4 difference between remote sensing and aircraft in-situ data is given. The statistical estimators are expressed in terms of bias and relative differences with respect to aircraft

Instruments	N Date (KST)	Bias ± std. (ppb)	Rel. diff. ± std. (%)
Aircraft vs. g-b FTS	2014-10-05		
	10:29:03–10:45:01	−14.60	−0.78
	10:46:10–11:00:01	−15.50	−0.83
	11:45:19–12:01:05	−13.00	−0.70
	13:23:10–13:38:21	−16.40	−0.88
	13:39:30–13:53:33	−13.70	−0.74
	14:23:46–14:48:23	−13.70	−0.74
	14:49:40–15:04:30	−10.30	−0.56
	2014-10-07		
	13:39:32–13:54:00	−8.00	−0.43
	13:54:15–14:09:07	−4.50	−0.24
	14:39:38–14:54:00	−8.70	−0.47
	15:55:32–15:10:00	−0.30	−0.56
	15:39:47–15:54:21	−6.50	−0.35
	15:39:40–15:54:00	−11.60	−0.63
	15:55:32–16:09:00	−11.00	−0.59
	2017-10-29		
	09:59:16–10:31:08	0.90	0.05
	10:31:09–11:03:24	4.90	0.26
	12:58:58–13:37:07	15.10	0.82
	13:37:07–14:19:40	−2.70	−0.14
	2017-11-12		
	11:12:20–11:38:01	14.40	0.78
	11:38:02–12:13:00	15.10	0.82
	14:14:46–14:45:55	16.50	0.89
	14:45:56–15:23:47	13.00	0.70
	4	−3.66 ± 11.50	−0.19 ± 0.61
Aircraft vs. GOSAT (NIES V0221)	Date		
	2012-10-17	4.53	0.25
	2012-10-18	2.40	0.13
	2014-10-05	−20.90	−1.13
	3	−4.65 ± 14.11	−0.42 ± 0.84

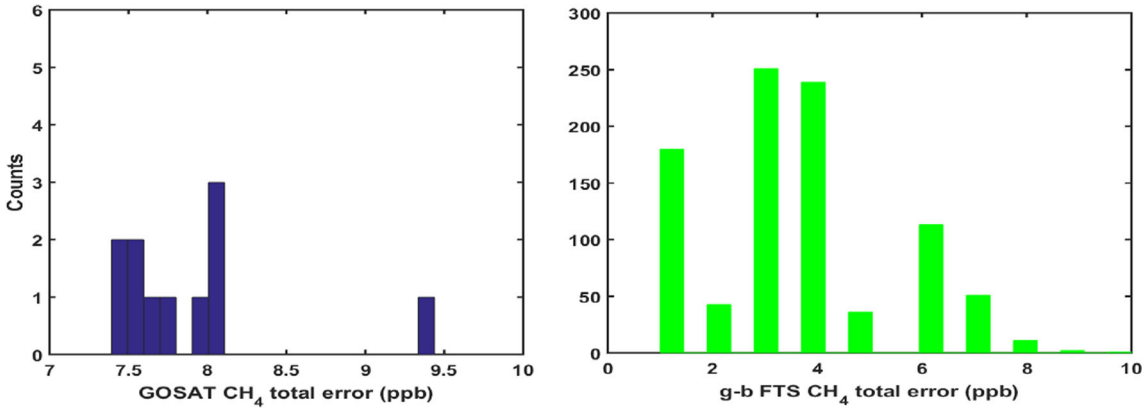

Fig. 9 The XCH_4 total errors are shown for GOSAT (left panel) and for g-b FTS (right panel). (It was displayed only for the coincident days)

tained near St. Petersburg, Russia and reported that the mean difference was -1.9 ± 14.5 ppb. Ohyama et al. (2015) reported that the average differences XCH_4 between TANSO-FTS and g-b FTS data (TANSO-FTS minus g-b FTS) is -7.6 ± 13.7 ppb. Right panel of Fig. 7 demonstrates the results of XCH_4 comparisons between the GOSAT and g-b FTS at the spatial coincidence criteria of ±1, ±3, ±5 degrees latitude/longitude green, blue, and red colors, respectively, and error bars indicate the standard deviations of the coincident datasets. This depicts that the GOSAT data is well consistent with the g-b FTS that lie on the best line. Therefore, we can infer that the impact the coincidence criteria (at least, up to ±5) for performing the comparison of XCH_4 over the Anmyeondo station is insignificant.

4.2 Aircraft XCH_4 Comparison with g-b FTS

Several aircraft observation campaigns over Anmyeondo site were carried out in the period between 2012 and 2017. However, a few numbers of aircraft data matched with the remote sensing instruments were available during this observation period. The g-b FTS XCH_4 was compared with the aircraft measurements. Here, g-b FTS data were averaged over a time window of ±30 min with respect to the aircraft measurement time. In addition, the averaging kernel of the g-b FTS was applied to the aircraft data to equalize the sensitivities of CH_4 mole fraction at each altitude for the total column. Wunch et al. (2010) reported that the airmass-dependent artifacts in XCH_4 due to spectroscopic inadequacies (e.g. line widths, inconsistencies in the relative strengths of weak and strong lines) in TCCON instruments were not seen. Here, a total number of the aircraft measurements that matched with g-b FTS were only four during the observation period of 2014 to 2017. The diurnal range of g-b FTS data reflects not only variability of airmass transport but source also sink processes and the effect of measurement errors as well (Keppel-Aleks et al. 2011). The overall results indicated that g-b FTS estimated slightly lower than aircraft. The statistical results for XCH_4 comparisons between aircraft and g-b FTS are shown in Fig. 8 and summarized in Table 3, (correlation coefficient was not computed because of small sample numbers). The mean absolute difference of XCH_4 between aircraft and g-b FTS is -3.66 ± 11.50 ppb, with a corresponding mean relative difference of $-0.19 \pm 0.69\%$. Previous findings have revealed that the unsampled part of the atmosphere above the aircraft ceiling contributes to the largest uncertainty in the total column calculated from the aircraft profiles (Wunch et al. 2010). We estimated the error contributions on aircraft-based XCH_4. The error components below the aircraft ceiling were derived by adding twice the precision of the aircraft data to the profile, and then re-integrated the profile (Wunch et al. 2010; Ohyama et al. 2015), the amount of error resulted in 3.03 ppb. The tropopause height variation induced an error of 0.40 ppb on averaged in estimating aircraft XCH_4 and the stratospheric error contribution were estimated by vertical shifting of the a priori by 1.0 km. That resulted in 6.30 ppb change on the aircraft XCH_4 values. The total errors were estimated to be 7.0 ppb (Table 4).

Table 4 Error budget for the estimated aircraft measurement of XCH_4. The total error is the sum, in quadrature, of the three errors. The aircraft error was estimated by adding the precision of the aircraft measurements to the profile and re-integrated the profile. Tropopause error was determined by varying 1.0 km, while stratospheric error was estimated by shifting the stratospheric apriori profile of CH_4 by 1.0 km. The fourth row on the given table shows the average value of the total retrieval errors from individual sounding of XCH_4 from g-b FTS and GOSAT

Aircraft error	Tropopause error	Stratospheric error	Total
3.03 ppb	0.40 ppb	6.30 ppb	7.00 ppb
g-b FTS total retrieval error		GOSAT total retrieval error	
3.60 ppb		7.70 ppb	

4.3 Aircraft XCH_4 Comparison with GOSAT

In this section, the comparison of the GOSAT retrieval product (V02.xx) of XCH_4 against the aircraft observations over the Anmyeondo station was analyzed. Based on the coincidence criteria, we obtained only three coincident days of observations. We took the mean values when obtaining more than one GOSAT measurements. As noted the aircraft data was smoothed by GOSAT column averaging kernels. The comparison results of XCH_4 between aircraft and GOSAT revealed a better agreement. The mean absolute difference of XCH_4 was about -4.65 ± 14.11 ppb, also shown in Table 3. The absolute value of XCH_4 difference on 5 October, 2014 was 20.9 ppb, which is larger than the other two coincident dates despite the fact that the matching data were observed on the closest time window. The discrepancy occurred at this particular date significantly affected the mean of difference and standard deviations. The difference could be attributable to the CH_4 variability in the lower atmosphere, the effect of aerosols/cirrus (Ohyama et al. 2015), or the large interval between air sampling levels, which is not sufficient to be captured the thin-layered structure of CH_4 profiles by GOSAT. We tried to look at atmospheric condition and aerosols during 5th October, 2015 using the information obtained from COMIS.4 (http://uis.comis4.kma.go.kr/comis4/uis/common/index.do#), Cloud-Aerosol Lidar and Infrared Pathfinder Satellite Observations (CALIPSO), and Aerosol Robotic Network (AERONET) (see Appendix Figs. 10, 11, and 12). However, we noticed tropospheric aerosols that might be suggesting that it tends to cause an underestimation of XCH_4 retrievals. Still further investigation is required in the future. However, the overall mean bias shown here is consistent with the previous results reported by Inoue et al. (2014, 2016). Inoue et al. (2014) made a comparison of GOSAT XCH_4 (V02.00) with 3 aircraft measurements from Yakutsk, Siberia and reported that the bias was 9.2 ± 15.2 ppb (3.7 ± 16.7 ppb) within ±2° (±5°). When considering 2 days average excluding a date of October 05, 2014, we obtained a bias 3.47 ± 1.51 ppb, which is agreed with Inoue et al. (2016) who showed a 4.5 ± 15.20 ppb over land. Fig. 4 shows the total retrieval errors (the room sum of the squares of smoothing error, retrieval noise, and interference error components) of XCH_4 obtained from GOSAT and g-b FTS. The standard deviation of the differences that we obtained here is slightly larger than the total estimated error of GOSAT (see Fig. 9 and Table 4) and the aircraft XCH_4. Further work is still required to have more robust conclusion by increasing the sample numbers.

5 Conclusions

Evaluating measurement of GHGs derived from multi-platform instruments against accurate and precise instrument such as aircraft in-situ is very essential when utilizing remote sensing GHGs results for source/sink estimations with inverse modeling. The results of the inverse models are very sensitive even to small biases in the data (Rayner and O'Brien 2001). In this work, we carried out the comparison of XCH_4 between g-b FTS and GOSAT over the Anmyeondo station. Based on the comparison results between g-b FTS and GOSAT, both instruments are generally well captured the seasonal variability of XCH_4, the maximum and minimum amount of methane was observed during summer and winter seasons, respectively. The overall results indicate that a relatively high variability was exhibited during a peak methane season. In addition, the impact the coincidence criteria was assessed and there was no systematic difference was observed. The bias was estimated to be from 0.1 to 3.37 ppb, and standard deviation was from 4.92 to 12.54 ppb. Column-averaged dry air mole fraction of CH_4 from 2012 to 2017 over the Anmyeondo station were derived by using CH_4 profiles measured by aircraft. Aircraft measurements have good accuracy, but are limited in altitude floor and ceiling, and so we have to use additional information for surface and the stratosphere. As to my knowledge, this is the first report on evaluation of remote sensing observations based on aircraft in-situ measurements of XCH_4 over this station. The uncertainty analysis of the aircraft measurements of XCH_4 confirmed the suitability of data for evaluating the remote sensing products. These in-situ observations of the target species were compared against g-b FTS, and GOSAT over there. It is noted that the averaging kernels of the remote sensing instruments were applied into the aircraft measurements. The retrieved XCH_4 values from the g-b FTS and GOSAT measurements showed a better agreement with the aircraft in-situ observations. Both instruments revealed a negative bias against aircraft. The relative differences of XCH_4 were found to be $-0.19 \pm 0.69\%$ and $-0.42 \pm 0.84\%$ with respect to g-b FTS and GOSAT, respectively. The small number of coincidences considered here hinders more robust conclusions, so we recommend to carry out further works on validation by taking more coincident data using in-situ and remote sensing instruments, as well as combining the model simulations in the future. This will allow us to improve clear identification of all the potential sources of uncertainties, as well as to understand the role of local source/sink and dynamics.

Acknowledgements This research was supported by the Research and Development for KMA Weather, Climate, and Earth system Services Support to use of Meteorological Information and value Creation (KMA-2018-00122). We acknowledge for those who provide the access for in-situ data from World Data Centre for Greenhouse Gases (WDCGG) (https://ds.data.jma.go.jp/gmd/wdcgg/cgi-bin/wdcgg/catalogue.cgi). We also greatly acknowledge the GOSAT science teams for the satellite data used in this work. Many thanks goes to the science teams for the provision of ECMWF ERA-interim and NOAA NCAR reanalysis data utilized in this study.

Appendix

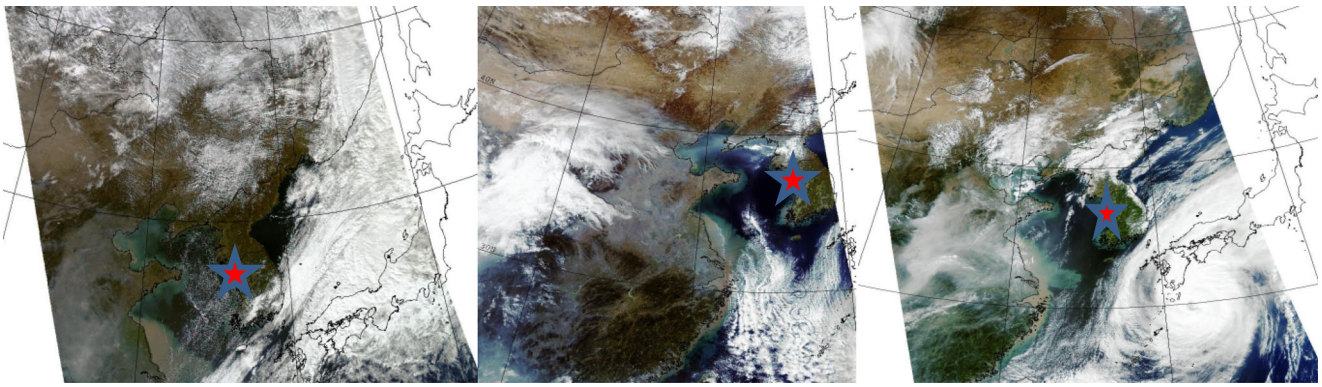

Fig. 10 Atmospheric sky conditions for 17th, 18th Oct. 2012, and 5th Oct. 2014, left to right panels, respectively, from COMIS.4. Red star shows Anmyeondo site. (http://uis.comis4.kma.go.kr/comis4/uis/common/index.do#)

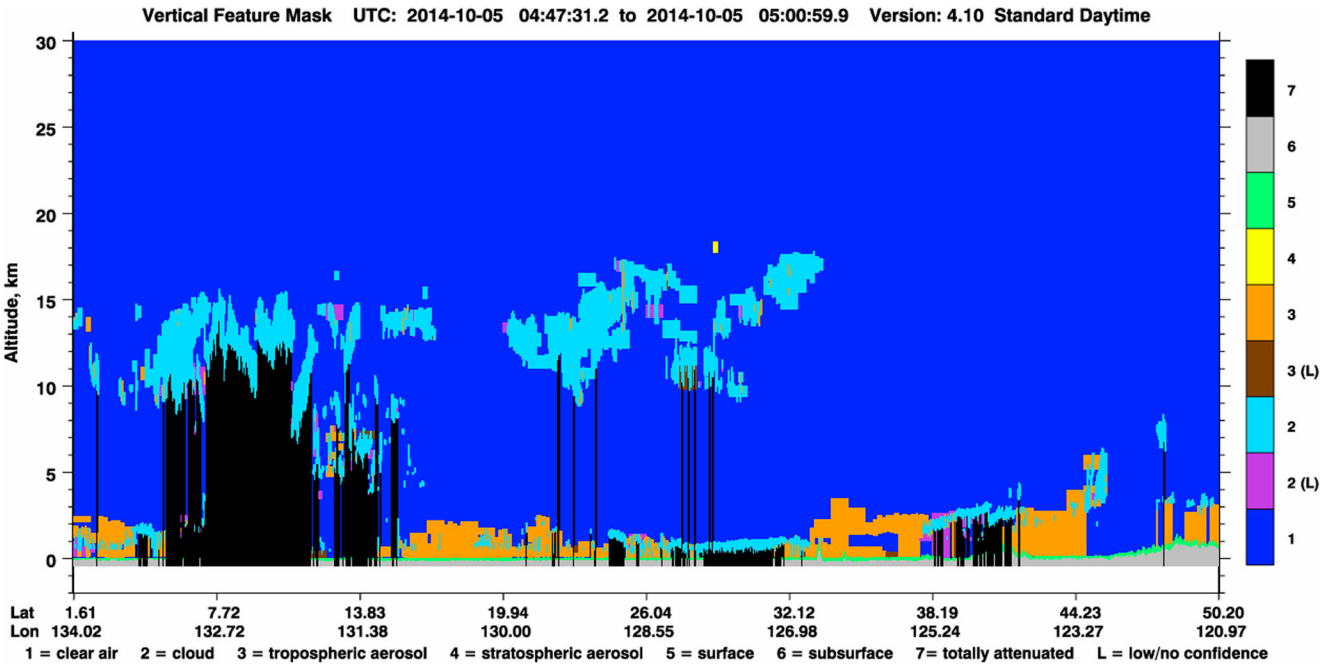

Fig. 11 Cloud and aerosol information from CALIOP data

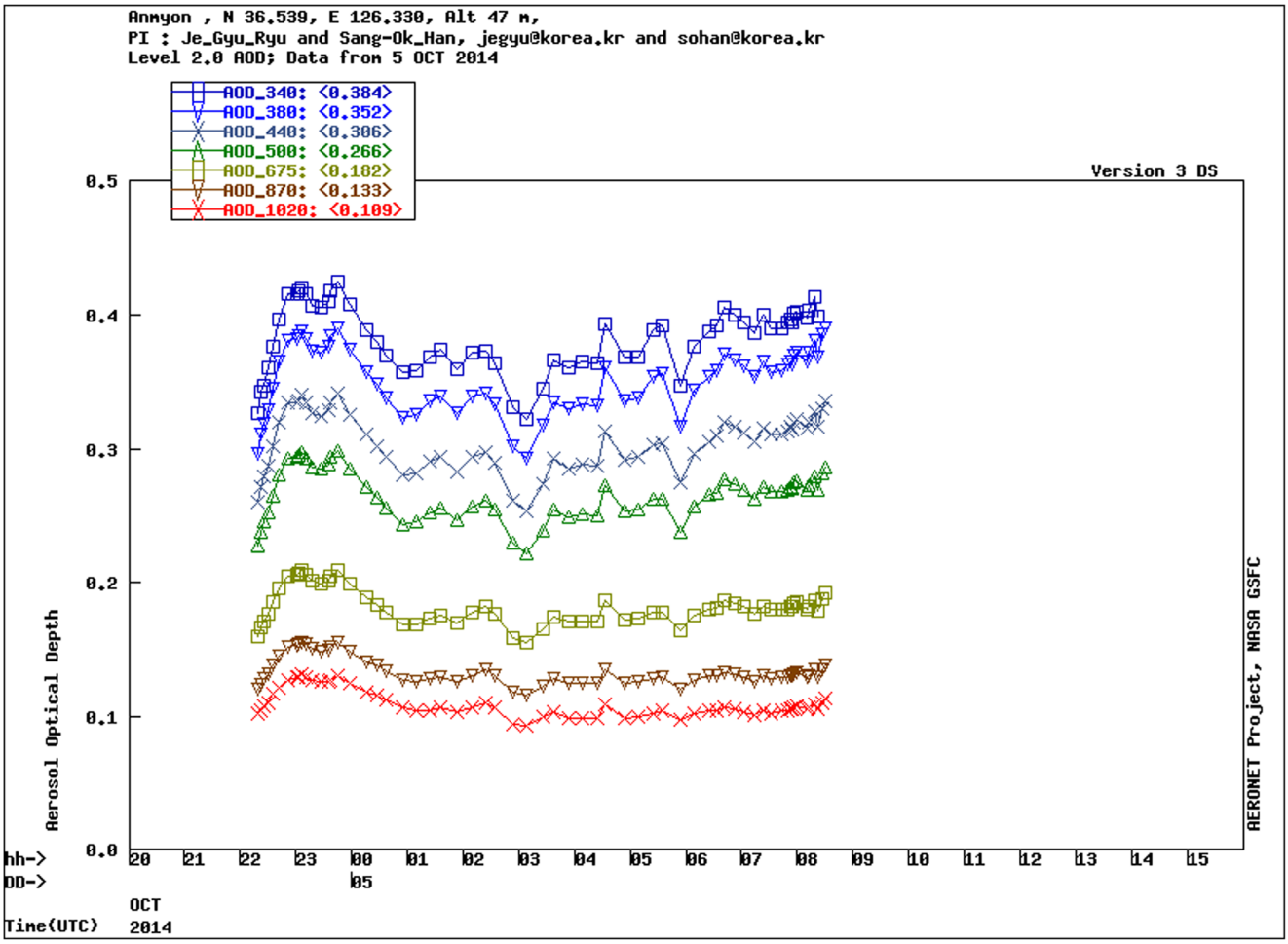

Fig. 12 Aerosol Optical Depth (AOD) from AERONET Level 2.0 data during 5th October, 2014 over Anmyeondo

References

Araki, M., Morino, I., Machida, T., Sawa, Y., Matsueda, H., Ohyama, H., Yokota, T., Uchino, O.: CO_2 column-averaged volume mixing ratio derived over Tsukuba from measurements by commercial airlines. Atmos. Chem. Phys. **10**, 7659–7667 (2010). https://doi.org/10.5194/acp-10-7659-2010.

Buchwitz, M., B. Dils, H. Boesch, C. Crevoisier, D. Detmers, C. Frankenberg, O. Hasekamp, W. Hewson, A. Laeng, S. Nol, J. Notholt, R. Parker, M. Reuter, and O. Schneising, 2016: ESA Climate Change Initiative (CCI) Product Validation and Intercomparison Report (PVIR) for the Essential Climate Variable (ECV) Greenhouse Gases (GHG) for data set Climate Research Data Package No. 3 (CRDP3), Version 4.0, 24. Feb. 2016.

Buchwitz, M., Schneising, O., Reuter, M., Heymann, J., Krautwurst, S., Bovensmann, H., Burrows, J.P., Boesch, H., Parker, R.J., Somkuti, P., Detmers, R.G., Hasekamp, O.P., Aben, I., Butz, A., Frankenberg, C., Turner, A.J.: Satellite-derived methane hotspot emission estimates using a fast data-driven method. Atmos. Chem. Phys. **17**, 5751–5774 (2017). https://doi.org/10.5194/acp-17-5751-2017

Chen, H., Winderlich, J., Gerbig, C., Hoefer, A., Rella, C.W., Crosson, E.R., Van Pelt, A.D., Steinbach, J., Kolle, O., Beck, V., Daube, B.C., Gottlieb, E.W., Chow, V.Y., Santoni, G.W., Wofsy, S.C.: High accuracy continuous airborne measurements of greenhouse gases (CO_2 and CH_4) using the cavity ring-down spectroscopy (CRDS) technique. Atmos. Meas. Tech. **3**, 375–386 (2010)

Cicerone, R.J., Oremland, R.S.: Biogeochemical aspects of atmospheric methane. Glob. Biogeochem. Cycles. **2**, 299–327 (1988)

Dlugokencky, E.J., Haris, J.M., Chung, Y.S., Tans, P.P., Fung, I.: The relationship between the methane seasonal cycle and regional sources and sinks at Tae-ahn peninsula, Korea. Atmos. Environ. Part A. **27**, 2015–2120 (1993)

Dlugokencky, E.J., Steele, L.O., Lang, P.M., Masarie, K.A.: The growth rate and distribution of atmospheric methane. J. Geophys. Res. **99**, 1702117044 (1994). https://doi.org/10.1029/94JD01245.

Frankenberg, C., Bergamaschi, P., Butz, A., Houweling, S., Meirink, J.F., Notholt, J., Petersen, A.K., Schrijver, H., Warneke, T., Aben, I.: Tropical methane emissions: a revised view from SCIAMACHY onboard ENVISAT. Geophys. Res. Lett. **35**, L15811 (2008). https://doi.org/10.1029/2008GL034300

Gavrilov, N.M., Makarova, M.V., Poberovskii, A.V., Timofeyev, Y.M.: Comparisons of CH4 ground-based FTIR measurements near Saint Petersburg with GOSAT observations. Atmos. Meas. Tech. **7**, 1003–1010 (2014). https://doi.org/10.5194/amt-7-1003-2014

Geibel, M.C., Messerschmidt, J., Gerbig, C., Blumenstock, T., Chen, H., Hase, F., Kolle, O., Lavrič, J.V., Notholt, J., Palm, M., Rettinger, M., Schmidt, M., Sussmann, R., Warneke, T., Feist, D.G.: Calibration of column-averaged CH_4 over European TCCON FTS sites with airborne in-situ measurements. Atmos. Chem. Phys. **12**, 8763–8775 (2012)

Houweling, S., Dentener, F., Lelieveld, J.: Simulation of preindustrial atmospheric methane to constrain the global source strength of natural wetlands. J. Geophys. Res. **105**, 17243–17255 (2000)

Inoue, M., Morino, I., Uchino, O., Miyamoto, Y., Yoshida, Y., Yokota, T., Machida, T., Sawa, Y., Matsueda, H., Sweeney, C., Tans, P.P., Andrews, A.E., C, S., Biraud, T., Tanaka, S.K., Patra, P.K.: Validation of XCO_2 derived from SWIR spectra of GOSAT TANSO-FTS with aircraft measurement data. Atmos. Chem. Phys. **13**, 97719788–97719788 (2013). https://doi.org/10.5194/acp-13-9771-2013

Inoue, M., Morino, I., Uchino, O., Miyamoto, Y., Saeki, T., Yoshida, Y., Yokota, T., Sweeney, C., Tans, P.P., Biraud, S.C., Machida, T., Pittman, J.V., Kort, E.A., Tanaka, T., Kawakami, S., Sawa, Y., Tsuboi, K., Matsueda, H.: Validation of XCH_4 derived from SWIR spectra of GOSAT TANSO-FTS with aircraft measurement data. Atmos. Meas. Tech. **7**, 2987–3005 (2014). https://doi.org/10.5194/amt-7-2987-2014.

Inoue, M., I. Morino, O. Uchino, T. Nakatsuru, Y. Yoshida, T. Yokota, D. Wunch, P. O. Wennberg, C. M. Roehl, D. W. T. Griffith, V. A. Velazco, N. M. Deutscher, T. Warneke, J. Notholt, J. John Robinson, V. Sherlock, F. Hase, T. Blumenstock, M. Rettinger, R. Sussmann, E. Kyr, R. Kivi, K. Shiomi, S. Kawakami, M. De Mazire, S. G. Arnold, D. G. Feist, E. A. Barrow, J. James Barney, M. Dubey, M., Schneider, L. T. Iraci, J. R. Podolske, P. W. Hillyard, T. Machida, Y. Sawa, K. Tsuboi, H. Matsueda, C. Sweeney, P. P. Tans, A. E. Andrews, S. C. Biraud, Y. Fukuyama, J. V. Pittman, E. A. Kort, and T. Tanaka, 2016: Bias corrections of GOSAT SWIR XCO_2 and XCH_4 with TCCON data and their evaluation using aircraft measurement data. Atmos. Meas. Tech., 9, 34913512.

Jain, A.K., Briegleb, B.P., Minschwaner, K., Wuebbles, D.J.: Radiative forcing and global warming potentials of 39 greenhouse gases. J. Geophys. Res. **105**(D16, 380 August 27), 20773–20790 (2000)

Keppel-Aleks, G., Wennberg, P.O., Schneider, T.: Sources of variations in total column carbon dioxide. Atmos. Chem. Phys. **11**, 3581–3593 (2011). https://doi.org/10.5194/acp-11-3581-2011.

Kuze, A., Suto, H., Nakajima, M., Hamazaki, T.: 2009: thermal and near infrared sensor for carbon observation Fourier-transform spectrometer on the greenhouse gases observing satellite for greenhouse gases monitoring. Appl. Opt. **48**, 6716–6733 (2009)

Messerschmidt, J., Geibel, M.C., Blumenstock, T., Chen, H., Deutscher, N.M., Engel, A., Feist, D.G., Gerbig, C., Gisi, M., Hase, F., Katrynski, K., Kolle, O., Lavric, J.V., Notholt, J., Palm, M., Ramonet, M., Rettinger, M., Schmidt, M., Sussmann, R., Toon, G.C., Truong, F., Warneke, T., Wennberg, P.O., Wunch, D., Xueref-Remy, I.: Calibration of TCCON column-averaged CO_2: the first aircraft campaign over European TCCON sites. Atmos. Chem. Phys. **11**, 1076510777–1076510777 (2011). https://doi.org/10.5194/acp-11-10765-2011

Miyamoto, Y., Inoue, M., Morino, I., Uchino, O., Yokota, T., Machida, T., Sawa, Y., Matsueda, H., Sweeney, C., Tans, P.P., Andrews, A.E., Patra, P.K.: Atmospheric column-averaged mole fractions of carbon dioxide at 53 aircraft measurement sites. Atmos. Chem. Phys. **13**, 52655275 (2013)

Morino, I., Uchino, O., Inoue, M., Yoshida, Y., Yokota, T., Wennberg, P.O., Toon, G.C., Wunch, D., Roehl, C.M., Notholt, J., Warneke, T., Messerschmidt, J., Griffith, D.W.T., Deutscher, N.M., Sherlock, V., Connor, B., Robinson, J., Sussmann, R., Rettinger, M.: Preliminary validation of column-averaged volume mixing ratios of carbon dioxide and methane retrieved from GOSAT short-wavelength infrared spectra. Atmos. Meas. Tech. **4**, 1061–1076 (2011). https://doi.org/10.5194/amt-4-1061-2011.

Oh, Y.-S., Kenea, S.T., Goo, T.-Y., Chung, K.-S., Rhee, J.-S., Ou, M.-L., Byun, Y.-H., Paul Wennberg, O.P.P., Kiel, M., DiGangi, J.P., Diskin, G.S., Velazco, V.A., Griffith, D.W.T.: Characteristics of greenhouse gas concentrations derived from ground-based FTS spectra at Anmyeondo, South Korea. Atmos. Meas. Tech. **11**(1–14), 2018 (2018)

Ohyama, H., Kawakami, S., Tanaka, T., Morino, I., Uchino, O., Inoue, M., Sakai, T., Nagai, T., Yamazaki, A., Uchiyama, A., Fukamachi, T., Sakashita, M., Kawasaki, T., Akaho, T., Arai, K., Okumura, H.: Observations of XCO_2 and XCH_4 with ground-based high-resolution FTS at Saga, Japan, and comparisons with GOSAT products. Atmos. Meas. Tech. **8**, 5263–5276 (2015)

Rayner, P.J., O'Brien, D.M.: The utility of remotely sensed CO_2 concentration data in surface source inversions. Geophys. Res. Lett. **28**, 175178 (2001)

Rodgers, C. D. 2000: Inverse methods for atmospheric sounding: Theory and Practic, World Scientific Publishing Co. Pte. Ltd, Singapore, ISBN-10: 981–02-2740-X.

Rodgers and Connor: Intercomparison of remote sounding instruments. J. Geophys. Res. **108**(405), 4116 (2003). https://doi.org/10.1029/2002JD002299

Tanaka, T., Miyamoto, Y., Morino, I., Machida, T., Nagahama, T., Sawa, Y., Matsueda, H., Wunch, D., Kawakami, S., Uchino, O.: Aircraft measurements of carbon dioxide and methane for the calibration of ground-based high-resolution Fourier transform spectrometers and a comparison to GOSAT data measured over Tsukuba and Moshiri. Atmos. Meas. Tech. **5**, 20032012–20032012 (2012). https://doi.org/10.5194/amt-5-2003-2012

Wunch, D., Toon, G.C., Wennberg, P.O., Wofsy, S.C., Stephens, B.B., Fischer, M.L., Uchino, O., Abshire, J.B., Bernath, P., Biraud, S.C., Blavier, J.-F.L., Boone, C., Bowman, K.P., Browell, E.V., Campos, T., Connor, B.J., Daube, B.C., Deutscher, N.M., Diao, M., Elkins, J.W., Gerbig, C., Gottlieb, E., Griffith, D.W.T., Hurst, D.F., Jimnez, R., Keppel-Aleks, G., Kort, E.A., Macatangay, R., Machida, T., Matsueda, H., Moore, F., Morino, I., Park, S., Robinson, J., Roehl, C.M., Sawa, Y., Sherlock, V., Sweeney, C., Tanaka, T., Zondlo, M.A.: Calibration of the Total carbon column observing network using aircraft profile data. Atmos. Meas. Tech. **3**, 13511362–13511362 (2010). https://doi.org/10.5194/amt-3-1351-2010

Wunch, D., Toon, G.C., Blavier, J.-F.L., Washenfelder, R.A., Notholt, J., Connor, B.J., Griffith, D.W.T., Sherlock, V., Wennberg, P.O.: The Total carbon column observing network. Philos. T. R. Soc. A. **369**, 20872112–20872112 (2011). https://doi.org/10.1098/rsta.2010.0240

Yang, Z., Washenfelder, R.R., Keppel-Aleks, G., Krakauer, N., Randerson, J., Tans, P., Sweeney, C., Wennberg, P.: New constraints on northern hemisphere growing season net flux. Geophys. Res. Lett. **34**, L12807 (2007). https://doi.org/10.1029/2007GL029742

Yoshida, Y., Ota, Y., Eguchi, N., Kikuchi, N., Nobuta, K., Tran, H., Morino, I., Yokota, T.: Retrieval algorithm for CO_2 and CH_4 column abundances from short-wavelength infrared spectral observations by the greenhouse gases observing satellite. Atmos. Meas. Tech. **4**, 717–734 (2011). https://doi.org/10.5194/amt-4-717-2011

Yoshida, Y., Kikuchi, N., Morino, I., Uchino, O., Oshchepkov, S., Bril, A., Saeki, T., Schutgens, N., Toon, G.C., Wunch, D., Roehl, C.M., Wennberg, P.O., Griffith, D.W.T., Deutscher, N.M., Warneke, T., Notholt, J., Robinson, J., Sherlock, V., Connor, B., Rettinger, M., Sussmann, R., Ahonen, P., Heikkinen, P., Kyr, E., Mendonca, J., Strong, K., Hase, F., Dohe, S., Yokota, T.: Improvement of the retrieval algorithm for GOSAT SWIR XCO_2 and XCH_4 and their validation using TCCON data. Atmos. Meas. Tech. **6**, 1533–1547 (2013). https://doi.org/10.5194/amt-6-1533-2013.